Sputtering of gold by fast neutrons

M. A. Kirk, R. A. Conner, and D. G. Wozniak
Materials Science Division, Argonne National Laboratory, Argonne, Illinois 60439

L. R. Greenwood, R. L. Malewicki, and R. R. Heinrich
Chemical Engineering Division, Argonne National Laboratory, Argonne, Illinois 60439

(Received 26 June 1978)

Experiments on the sputtering of single-crystal gold by fast neutrons at temperatures less than 40 K are reported. Prior thermal-neutron activation of the gold crystals permitted a determination of the spatial distribution of sputtered atoms by autoradiography. Sputtering yields were determined by γ counting. The neutron flux and energy spectrum were determined and damage parameters were calculated for gold. An average sputtering ratio of 8.0×10^{-6} sputtered gold atoms per incident neutron ($E > 0.1$ MeV) was found with an uncertainty of $\pm 34\%$. The spatial distribution of sputtered atoms was found to be very nearly random. The present experiment is compared in detail with other fast-neutron sputtering experiments and theories.

I. INTRODUCTION

The sputtering or ejection of surface atoms by high-energy-particle irradiation has been the subject of considerable experimental investigation for about 20 years. The majority of sputtering experiments have involved the bombardment of metal surfaces with energetic ions. The basis for much of our interest in sputtering has been the recognized close connection between the physics of sputtering and the physics of radiation-damage phenomena in the bulk. The recoil cascade that produces a distribution of vacancies and interstitials in the bulk can also produce sputtering when that cascade occurs near the surface. The experimental investigation of sputtering is a unique tool with which to study the physics of defect cascade formation, a process of very short duration (10^{-13}–10^{-11} sec).

Very little previous work has been accomplished on the sputtering of solids by fast-neutron bombardment. Recently, however, a number of sputtering experiments have been performed with 14-MeV neutrons in order to gain insight into potential technological problems associated with the containment vessel wall of future nuclear-fusion reactors. The lack of agreement among previous experimental results on both fission- and fusion-neutron sputtering, and the limited accuracy of individual measurements, have been discouraging. The experimentally determined sputtering ratios (number of sputtered atoms per incident neutron) for gold, a widely studied metal, have ranged over three orders of magnitude. The major factors that interfere with the accurate determination of sputtering yield in a neutron-radiation environment are the low signal-to-background ratio and the contamination problems associated with the measurement of extremely small quantities (10^{10}–10^{13} atoms) of an element. These problems have been especially severe in sputtering experiments with 14-MeV neutrons, where the neutron-source strength (and hence sputtering yield) is typically two or more orders of magnitude below that of a fission-neutron source.

We are primarily interested in sputtering as a means to investigate mechanisms of radiation-damage production during fission-neutron bombardment. We have investigated focused collision sequences and other possible mechanisms for directional sputtering; the intersection of high-energy recoil cascades with the surface as a mechanism for direct sputtering, and the contribution to sputtering of the so-called thermal-spike mechanism.

Single-crystal gold was chosen as the material for the present study for several reasons. Single crystals were used to detect sputtering that might take place along major crystalline directions. Gold was chosen because it lacks a significant oxide layer and because it has been used in most previous work on neutron sputtering. Gold possesses convenient nuclear properties for the application of neutron-activation analysis techniques. The techniques employed in most previous neutron sputtering experiments involve neutron activation of the sputtered and collected atoms along with the collector material during or following the sputtering irradiation. However, high background levels from the activated collector can give misleading results and make a determination of the spatial distribution of sputtered and collected atoms virtually impossible. This was found to be the case in our earliest published work on the neutron sput-

tering of gold.[1] For these reasons a technique of preactivation of the gold crystal was developed. This method permitted a far more accurate determination of the sputtering yield and resulted in good autoradiographic data on the spatial distribution of sputtered gold atoms. An important and unique feature of the fast-neutron facility is the extremely low thermal-neutron flux, which results in sputtering with a minimum amount of background neutron activation. This has led to the first picture of its kind illustrating the spatial distribution of atoms sputtered by fast neutrons. Some of this work has already been reported in a preliminary form.[2]

The current work required a highly accurate determination of the neutron flux and energy spectrum for the low-temperature fast-neutron-irradiation facility in which these studies were performed. This was accomplished, and neutron damage parameters based on the neutron spectrum were also calculated for many elements of interest. These damage parameters include the spectrum-averaged total recoil cross section, primary recoil distribution, spectrum-averaged total damage-energy cross section (with electronic losses calculated and subtracted), and damage-energy distribution. These data have proven valuable not only for the analysis of the present sputtering work, but also for the other irradiation experiments performed in this facility. The results of the neutron flux and energy spectrum determination, and the damage parameters calculated for gold, are included in the present report. This information has permitted meaningful comparisons between the present work and many of the previous experiments at other neutron sources, and a more detailed comparison with theoretical models than was previously possible.

II. EXPERIMENTAL METHODS

A. Sputtering

Single crystals of gold were grown from high-purity (99.9999%) starting material (Cominco Electronic Materials) in graphite crucibles under an argon atmosphere by the Bridgman technique. The crystals were cylindrical (6.4 mm in diameter and 6.4 mm in length) and grown with a tail to permit mechanical connection to a crystal holder. The cylindrical as-grown surface was heavily electropolished, removing ~20 μm, and the crystals were then annealed in air at 900 K for 1–2 h. The surface was examined by scanning electron microscopy, and appeared smooth on a 0.1-μm scale, with slight vertical undulations on a 10-μm scale.

Schematics of the crystal holder, activation capsule, and sputtering capsule are shown in Fig. 1. All components were made of commercial high-purity aluminum, chemically etched and well annealed. All joints were electron-beam welded. The design of the crystal holder and capsules allowed evacuation, good heat transfer between crystal and capsule, and remote crystal transfer from activation to sputtering capsule without contact between the crystal and any walls.

Activation of the gold crystal took place in a D_2O-cooled core position in the CP-5 reactor at Argonne National Laboratory. The total neutron flux in this position is ~1×10^{18} neutrons/m^2 sec

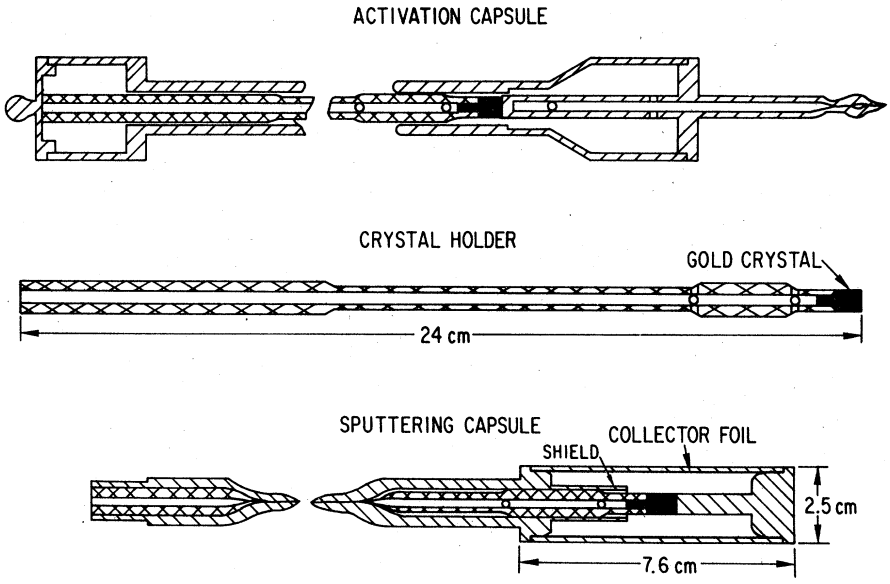

FIG. 1. Schematics of activation capsule, gold-crystal holder, and sputtering capsule.

with a cadmium ratio of 3. The estimated crystal temperature during activation was between 323 and 373 K. The activation period ranged from 13 to 20 days; this yielded >95% of saturation activity with an active atomic fraction of 0.001. At the end of activation, the gold activity was 1000 Ci (or $\sim 10^7$ R/h at the surface). This extreme radiation hazard necessitated handling in heavy casks and remote manipulation in a hot cell. Special cutting, handling, and crimping tools were developed to permit remote opening of the activation capsule and transfer of crystal and holder to the sputtering capsule. In the last of three runs (run *C*) the gold crystal was annealed for 30 min at 723 K in the activation capsule prior to opening, in order to eliminate defect clusters in the radiation-damaged crystal. However, this annealing apparently had little or no influence on the results.

The sputtering capsule contained a single collector foil mechanically held against the inside circumference. This high-purity (99.99%), 2.54×10^{-2}-mm-thick aluminum foil (supplied by Goodfellows Metals, Ltd., England) had lower gold-impurity level than other commercially available foils. Smaller pieces of foil, from the same stock from which the collector was cut, were packaged and attached to the outside of the sputtering capsules. These foils served as blanks for the determination of gold background in the foil activated by the sputtering irradiation. After the transfer of the activated crystal to the sputtering capsule, the latter was evacuated to a pressure of $\sim 10^{-3}$ Torr (0.13 Pa), baked out at 373 K for 30 min, and sealed by crimping and the use of a low-temperature radiation-resistant epoxy.

The sputtering irradiation took place in the low-temperature fast-neutron-irradiation facility in the CP-5 reactor. The desired sputtering fluence was achieved in about 4 days for all runs. Based on the linear increase in sputtering yield (and collection) with fluence and the exponential decay of radioactive gold atoms (2.7-d half-life), 4 days of sputtering irradiation gave the maximum yield of sputtered active gold atoms. The fluence for each run was measured by integration of a thermopile voltage that monitored reactor power. The calibration of this method (determination of neutron flux and energy spectrum) is discussed below. The temperature of the gold crystal during sputtering, measured in one run, was <40 K. The vacuum during irradiation was maintained at $\sim 10^{-6}$ Torr (0.13 mPa), or, better, by cryogenic pumping.[1] The γ-radiation-induced outgassing may be a beneficial effect in that it minimizes the amount of adsorbed gas on the gold crystal. For the γ flux level in this facility, approximately one gas monolayer is removed every 4–8 h.[3] With a crystal temperature of 40 K and a capsule temperature of 5 K, this outgassing would increase the probability of recondensation of gas atoms on capsule surfaces. The capsule was slowly cooled from 100 K with the reactor operating (crystal simultaneously cooled from ~140 K) at the beginning of each sputtering irradiation to take advantage of this effect.

Following the sputtering irradiation the gold crystal was removed from the sputtering capsule through the stem. The sputtering capsule was opened and the collector foil flattened and mounted between two developed film emulsions. About 1 month later a piece of the crystal tail was removed for precise determination of the fraction of active atoms.

B. Autoradiography

Autoradiographs of the collector foil were made with Kodak Medical No-Screen (MNS) and type-AA films. The collector-foil package and unexposed film were sandwiched between lead sheets and held tightly together in a film cassette. The major background radiation was due to ^{24}Na (produced by the Al(n, α) reaction), which has a 15-h half-life. Good resolution of the ^{198}Au (2.7-day half-life) distribution was usually obtained with reasonable (12–48 h) exposure times between 4 and 8 days after removal of the foil from the sputtering capsule. Beyond about 8 days, radiation from ^{198}Au became too weak for adequate exposures even with the faster film (MNS), and foils were then analyzed by γ counting, as discussed in Sec. IIC.

Figure 2 shows a positive print of an autoradiograph from the collector of run *A*. This radiograph was one of the best obtained, but was also typical of all three runs, except that in run *A* a longer shield was present near the crystal in the sputtering capsule (see Fig. 1). The asymmetric shadow effect of this longer shield can be observed in the radiograph and in the corresponding densitometer trace (Fig. 3). This shadow effect displays the distinctly geometrical nature of the sputtering and collection of sputtered atoms, and indicates that the sticking coefficient of the sputtered gold on the aluminum collector is nearly unity. Selected-area γ counting (discussed in Sec. IIC) showed that the central stripe and small bright spots in Fig. 2 were due to ^{198}Au radiation.

Autoradiographs from run *C* were similar to those from run *A*; again, a few small spots of contamination were observed. However, the gold distribution in run *C* fell off evenly above and below the central strip because of the shorter shield. The autoradiographs from run *B* revealed the same central stripe of ^{198}Au seen in the other runs,

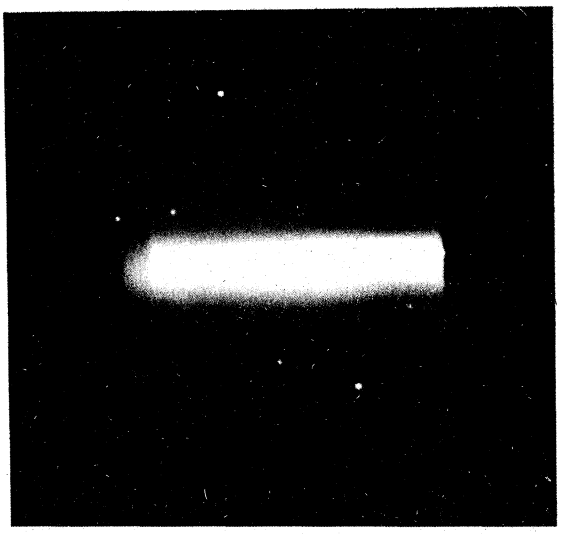

FIG. 2. Positive print of autoradiograph of collector foil from run *A* (cylindrical axis is vertical).

but showed more contamination. A blank run was also performed in which all procedures were carried out as in runs *A*–*C*, except the sputtering irradiation was omitted; the sputtering capsule and crystal remained in the hot cell for 4 days at room temperature. Autoradiographs from this control run revealed no central stripe of ^{198}Au,

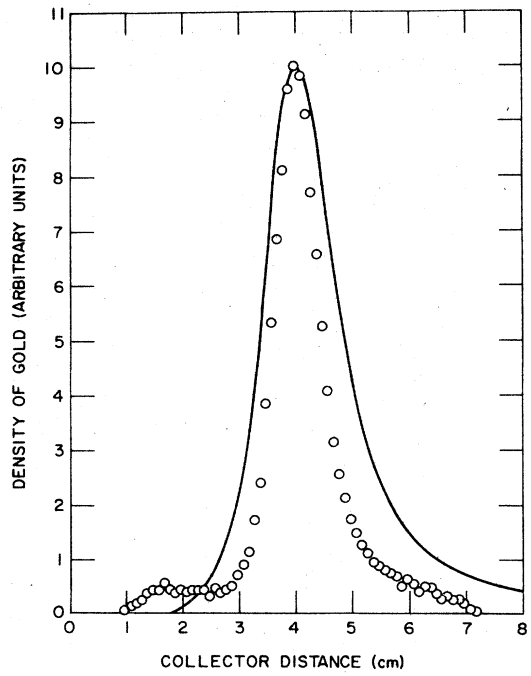

FIG. 3. Microphotodensitometer trace of autoradiograph from Fig. 2 (collector distance is along cylinder axis). The solid (theoretical) curve corresponds to directionally random sputtering.

but the large amount of contamination present on the collector prevented meaningful γ counting. These results showed that the ^{198}Au central stripe was due to neutron sputtering and the small spots of ^{198}Au were indeed due to contamination, probably produced by the handling and crimp-sealing operations. In most runs this contamination was minimal; in runs *A* and *C* it amounted to no more than 10% of the total yield.

Scanning microphotodensitometry was performed on the autoradiograph of Fig. 2. A set of scans covering the entire autoradiograph was performed in a search for a sputtering-spot pattern that might not be discernable to the naked eye. No such pattern was found. A typical single scan through the central stripe is displayed by the data points in Fig. 3. The solid line in Fig. 3 shows the random- sputtering distribution expected for the experimental crystal and collector geometry used in run *A*. This theoretical curve also takes into account the asymmetric shadow effect shown by the data and caused by the long shield. The background was estimated as a straight line to an accuracy of 5% in gold density. These data indicate that at least 85% of the sputtering was approximately random. Since the film-darkening and densitometer response were carefully calibrated to ^{198}Au radiation, the slight deviation of the experimental distribution from randomness is evidently a real effect.

C. Decay-γ counting

Following the autoradiographic work, the collectors and blank foils were analyzed for decay γ's by the Dosimetry Group of the Chemical Engineering Division at Argonne National Laboratory. Calibrated full foil counts were made with Ge(Li) detectors to determine ^{198}Au concentration. Usually, three or four counts were performed over several ^{198}Au half-lives, with count times sufficient to produce <2% statistical error in ^{198}Au disintegration rates for the 411.8-keV peak. Peak integration and Compton-background subtraction were done by computer.

The ^{198}Au background caused by the activation of gold impurity in the aluminum collector foils during the sputtering irradiation was determined from the blank foils and subtracted from the collector-foil activity. The remaining ^{198}Au activity on the collector was calibrated to yield total gold atoms sputtered. For this calibration a small piece of the crystal tail was flattened to reduce the γ self-absorption correction, and accurately weighed to determine the original fraction of activated atoms. The thermal- and resonance-neutron self-shielding correction for this piece was calcu-

TABLE I. Experimental sputtering yields, neutron fluence, and sputtering ratios for gold.

Run	Yield (gold atoms)	Fluence (neutrons, $E>0.1$ MeV)	Ratio (atoms/neutron)
A	7.09×10^{12} (±18%)	6.8×10^{17}	1.1×10^{-5} (±31%)
B	2.63×10^{13} (±11%)	1.0×10^{18}	2.5×10^{-5} (±27%)
C	4.67×10^{12} (±13%)	7.0×10^{17}	6.7×10^{-6} (±28%)

lated to be ≲20%. However, this correction was approximately offset by a somewhat larger neutron flux calculated to be present in the location of the small piece of the crystal tail. This is a result of self shielding by the bulk of the gold crystal. The uncertainty in these corrections yields an additional uncertainty in the calibration of the active fraction of gold at the sputtered surface of ±10%. The sensitivity of this experimental determination of sputtered gold atoms was limited by the gold-impurity background in the collector foils. This background level was always approximately one order of magnitude less than the activity due to the sputtered radioactive ^{198}Au.

The total yields of sputtered gold atoms for all three runs are shown in Table I. The yield for run *A* has been corrected by 20% for the shadow effect previously discussed.[4] The uncertainty quoted for each run is the cumulative error of the counting, peak integration, and Compton-background subtraction for three sources (collector, blank, and crystal piece), weighing of the crystal piece, and neutron self-shielding effects. All yields include the small spots of contamination evident (for example) in Fig. 2. For run *A*, counts of selected areas with NaI detectors showed that the central portion of the stripe contained 85% of the total ^{198}Au, and the major contamination spots

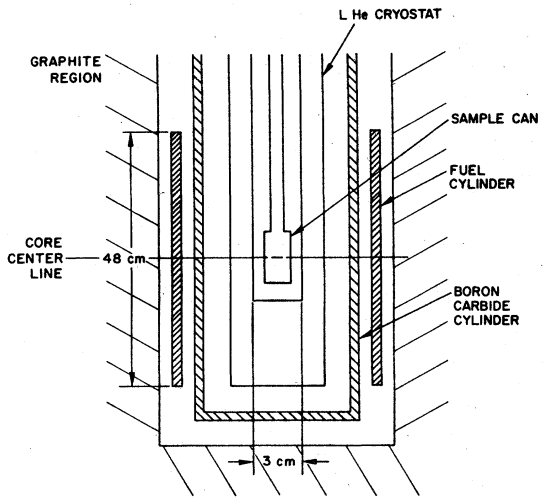

FIG. 4. Simplified schematic of the cryogenic fast-neutron-irradiation facility in CP-5.

<10%. An estimated ≳90% of the yield in run *A* is due to sputtering. Similar results were found for run *C*. However, run *B* had considerably more contamination than the other runs based on the autoradiographic evidence, and contamination activity for run *B*, could not be separated from sputtering activity. This, of course, could account for some or all of the differences in yield between run *B* and the other runs (Table I).

Also shown in Table I are the sputtering neutron fluences and resultant sputtering ratios. The error in sputtering ratios is the relative error based on the yield determinations and crystal surface areas. The absolute error would include the error in fluence which is not relevant to a comparison of these three runs. The fluence determination and its error are discussed in Sec. II D.

D. Neutron flux and energy spectrum

The interpretation of fast-neutron damage experiments, and comparisons between experiments performed at different irradiation facilities, require accurate information on the neutron flux and energy spectrum for each facility. Therefore, the present work includes a more precise determination of the neutron flux and energy spectrum than was previously available[5] for the low-temperature irradiation facility at CP-5. This information makes it possible to calculate with reasonable accuracy the spectrum-averaged total cross sections and distributions of primary recoil events and damage energies for various materials irradiated in the facility. The results of these calculations for gold will be discussed in Sec. III B.

Figure 4 shows a simplified schematic of the low-temperature fast-neutron-irradiation facility at CP-5 (a more detailed description is given in Ref. 6). This vertical thimble is located in the graphite reflector region surrounding the D_2O moderator tank, 1.2 m from the center of the reactor core of radius 0.3 m. The main elements displayed in this schematic are the Zircaloy-2+15-wt.% ^{235}U converter fuel cylinder (source of fission neutrons), boron carbide cylinder (thermal-neutron shield), simplified liquid-helium cryostat, and typical sample location.

To determine the neutron flux and energy spec-

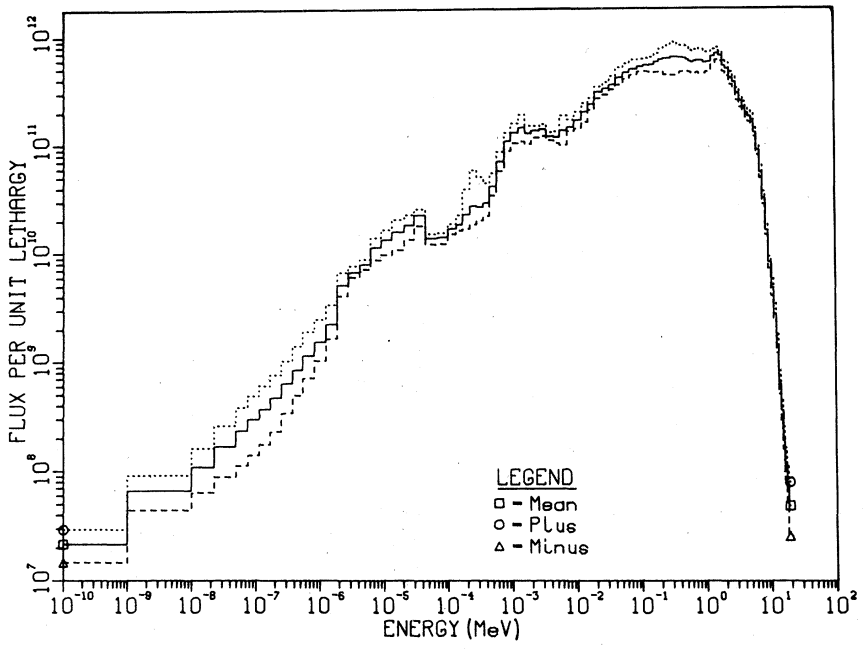

FIG. 5. Differential neutron-energy spectrum in lethargy units ± (one standard deviation).

trum, a package of 14 foils was located at the typical sample location. After irradiation, 20 foil activities were examined. The SAND II computer code[7] was used to iteratively determine the best neutron-spectrum fit to the 20 foil activities, corrected for self-absorption. A Monte Carlo routine was employed to produce standard-deviation errors in each neutron-energy group. The resultant covariant error matrix was also employed to generate the error in the differential recoil cross sections for various materials, and is displayed for gold in Sec. III B.

The differential neutron-energy spectrum in lethargy units (flux per logarithmic energy intervals) is shown in Fig. 5. The positive and negative single standard deviation spectra are also displayed. Some portions of the spectrum, notably between 0.1- and 1.0-MeV neutron energies, have relatively large errors due to a lack of sensitivity of foil reactions to neutrons in this energy region. Unfortunately no neutron reactions with a significant response within this region occur in any element. The bump in the spectrum near the 10^{-3}-MeV neutron-energy region is possibly due to fission neutrons from the converter, reflected back into the cryostat by the surrounding graphite.

Finally, the integrated flux for neutron energies greater than 0.11 MeV is 2.2×10^{16} neutrons/m^2 sec (±13%) with the reactor operating at 5 MW.

III. DISCUSSION

The autoradiograph of Fig. 2 represents the first experimental determination of the spatial distribution of atoms sputtered by fast neutrons. This claim was made previously by Garber *et al.*[8] in their work on the sputtering of a single-crystal gold foil by 14-MeV neutrons. However, an analysis of their gold foil, collector, and beam geometry reveals that the pattern they obtain cannot be due to directional sputtering at all. Also, it is very unlikely that autoradiography can resolve 6×10^{10} ^{198}Au atoms collected on an aluminum foil, with activation by a long thermal-neutron irradiation. Previous attempts[1,9] to resolve two orders of magnitude more ^{198}Au atoms collected on high-purity aluminum foil and high-purity quartz, and activated following sputtering, have failed because of excessive background activity.

Mention should be made of the experimental validity of the distribution of sputtered gold atoms shown by the photodensitometer data in Fig. 3. This experimental distribution is narrower than a theoretically random distribution. We believe that this is a real effect. Both the photodensitometer and the optical density of the film were carefully calibrated. The geometrical shadow effect displayed in Figs. 2 and 3 provides evidence both for a sticking coefficient of nearly unity for gold atoms on the aluminum collector and for a low probability of resputtering of the collected gold atoms. Also, distortion of the distribution pattern due to incomplete condensation does not occur for gold collected on cooled aluminum collectors.[10] Possible physical explanations for why the experimental sputtering distribution is narrower than a random distribution will be suggested later in the discussion.

Activation of the gold crystal prior to sputtering has thus facilitated the experimental resolution of the distribution of radioactive gold atoms on the collector. Since the collector foil is exposed only to the fast-neutron sputtering irradiation, background activity in the foil, including any gold-impurity activity in the collector foil itself, is minimized. This improves the accuracy of the sputtering yield determination. The use of a portion of the gold crystal to determine the active fraction is a convenient form of self-calibration and eliminates the need to determine the thermal-neutron flux independently. This avoids errors introduced by such factors as variations in thermal flux with position, changes in reactor configuration, and uncertain handling of activation at resonances.

The present autoradiographic technique also permits the direct observation of contamination on the collector foil. Contamination was found to some degree on all runs; two runs were not reported because autoradiographic evidence indicated too much contamination to make further analysis meaningful. Of the three runs reported here, only B was contaminated to the extent that the amount of contamination could not be estimated. The autoradiographs for runs A and C contained a few discrete spots of contamination, and the amount of contamination could be determined by selected-area counting. It should be emphasized that similar contamination was found on a blank run, implying that this is a result of handling procedures and not of the sputtering irradiation. The blank run did not show the central stripe produced by random sputtering.

A piece of gold about 2 μm in diameter contains 10^{12} atoms. An aluminum collector foil with the dimensions of our foil will contain $\geq 10^{14}$ gold-impurity atoms (10 ppb). These two facts can present serious experimental difficulties if activation techniques are employed, as they are in virtually all previous experiments. The background of gold in any particular technique must be determined, and in several previous experiments this was apparently done inadequately, if at all.

In order to compare the present results with those of other experiments and theories, a single value must be assigned to the sputtering ratio determined by the current experiments. Based on the autoradiographic evidence and the results of selected-area counting, only the data from runs A and C will be used. The average sputtering ratio for these two runs is $S = 8.9 \times 10^{-6}$, which is just within the relative experimental error of each run. In both runs, the contamination levels were ~10% of the total sputtering yields. Removing 10% from the average value of S gives $S = 8.0 \times 10^{-6}$ sputtered gold atoms per incident neutron ($E > 0.1$ MeV) with an uncertainty (including absolute flux error) of ±34%.

A. Comparison with other neutron-sputtering experiments

In order to meaningfully compare the results of various neutron-sputtering experiments, the differences in experimental geometries and neutron-energy spectra must be taken into account. This can be done by means of an expression similar to one derived by Sigmund[11] for the sputtering of a spherical sample in an isotropic fast-neutron flux:

$$S = 2g\Lambda N\langle\sigma T_d\rangle . \tag{1}$$

The factor $2g$ is a geometrical factor which we will adjust for the different experimental geometries. The material-dependent factors Λ and N will remain constant for all the sputtering experiments on gold. The damage-energy cross section or specific damage energy $\langle\sigma T_d\rangle$ will be determined for gold in the appropriate neutron-energy spectra, where possible.

Table II is a compilation of reported results for fast-neutron sputtering of gold.[12] Because of recent improvements in (d,T) and $d,\mathrm{Be})$ neutron experiments, only the most recent results employing these sources are included. The second column gives the sputtering ratios as originally reported. In the last column these ratios are normalized, by means of the Sigmund expression, to a spherical sample in an isotropic flux with the same damage-energy cross section found for gold in our facility ($E_n > 0.1$ MeV).[13] The geometrical factors used were as follows: The present results were multiplied by a factor of $\frac{3}{2}$ to account for our cylindrical geometry, in which sputtering from the cylinder-end surfaces was not permitted. Norcross *et al.*[14] and Fairand[9] employed foils in an isotropic flux, with collection on one side. They took one-half of the isotropic flux (correctly, but not for the reasons given in their papers) to calculate their sputtering ratios. To scale their sputtering ratios to a sphere in an isotropic flux, the full flux is used in the denominator with an additional factor of 2 in the numerator. These factors of 2 cancel. All the (d,T) and $d,\mathrm{Be})$ neutron experiments used foils in a beam. To obtain the spherical geometry in an isotropic flux, these ratios were scaled by a factor of 2.[10]

A few comments about the damage-energy cross sections shown in Table II are needed. The $\langle\sigma T_d\rangle$ for gold in our facility was calculated with the DISCS computer code of Odette and Doiron.[15] The neutron spectrum used by Fairand is described (and measured by seven nuclear reactions) as

TABLE II. Comparison of present work with some previous results of sputtering of gold by fast neutrons.

Authors	Reported yield (atoms/neutron)	Calculated damage-energy cross section (keV b)	Scaled yield (10^{-5} atoms/neutron)
	Fission neutrons [a]		
Kirk *et al.* (present work)	8.0×10^{-6} (±34%)	32.4[b]	1.2
Norcross *et al.*[c] (1966)	1.0×10^{-4} (±30%)		
Fairand[d] (1969)	1.2×10^{-4} (±30%)	47.7[e]	8.1
Verghese[f] (1969)	1.8×10^{-6} (±31%)	?	?
	14-MeV neutrons (d,T)		
Behrisch *et al.*[g] (1976)	2×10^{-4}–2×10^{-5}	217[h]	6.0–0.60
Harling *et al.*[i] (1976)	$\lesssim 1.9 \times 10^{-5}$ (±26%)	217	$\lesssim$0.57
	15-MeV neutrons (d,Be)		
Jenkins *et al.*[j] (1976)	2.8×10^{-5} (±29%)	198[k]	0.9
Harling *et al.*[i] (1976)	$\lesssim 1.9 \times 10^{-6}$ (±32%)	198	$\lesssim$0.06

[a] Yields for fluence of neutrons with $E > 0.1$ MeV except for the Verghese study in which $E > 1.0$ MeV.
[b] Calculated by DISCS code (Ref. 15) for neutron flux with $E > 0.1$ MeV.
[c] Reference 14.
[d] Reference 9.
[e] Calculated by DISCS code for pure-fission spectrum.
[f] Reference 17.
[g] These values are taken from Ref. 18; the higher yield is probably from Ref. 19, and the lower yield from Ref. 20.
[h] Calculated by DISCS code for 14.25-MeV neutrons.
[i] Reference 21.
[j] Reference 22.
[k] Reference 16.

having a pure-fission distribution for $E > 0.1$ MeV. Therefore, for Fairand's data, the $\langle \sigma T_d \rangle$ calculated for gold with the DISCS code employs the Cranberg fission spectrum.[23] The Norcross *et al.* spectrum was described[14] as a slightly softer spectrum than Fairand's, but the differences between these groups' results are minimal. (Fairand and Norcross *et al.* both used the Battelle Memorial Institute Research Reactor.) For the 14-MeV neutron experiments, $\langle \sigma T_d \rangle$ was calculated for gold with a 14.25-MeV monoenergetic source by means of the DISCS code. For the (d,Be) source, the value of $\langle \sigma T_d \rangle$ reported by Roberto *et al.*[16] for gold is given.

In comparing the normalized results for fission-neutron sputtering of gold we will only discuss our result and that of Fairand. The result of Norcross *et al.* is similar to Fairand's, and Verghese does not report his experimental methods or neutron flux in enough detail to permit a valid comparison. (The sputtering ratio reported by Verghese is, however, surprisingly low, especially for an integrated flux defined for neutron energies above 1.0 MeV.) Fairand's experimental methods differ from those of the current study in that he did not monitor contamination or measure the gold background introduced by impurities in the collector. Contamination may not have been a serious problem in Fairand's study, since the results of four different irradiations were reasonably close (S ranged from 0.8×10^{-4} to 1.5×10^{-5}). However, he interpreted his result as evidence of a very low sticking coefficient (~0.15) for gold atoms on quartz collectors. His result may, in fact, be due to a high gold background introduced by his collectors or gold-separation methods. Since we had an excellent monitor of contamination and made accurate gold-background determinations, we feel that our results are more accurate.

Contamination and high gold background in collectors have also been found in several experiments with 14-MeV neutron sources.[19,21] These problems are even more serious in experiments of this type, in which the amount of sputtered gold

on collectors is far less than in the fission-neutron experiments because of the limited neutron fluences available. This is reflected in the wide range of results for all (d,T) and (d,Be) neutron experiments, as reviewed by Behrisch[18] and Harling *et al.*[21] Only the most recent, and apparently most accurate, of these experiments are included in Table II for comparison. The normalized yields from the present fission-neutron study, the Harling *et al.* (d,T) neutron study, the Jenkins *et al.* (d,Be) neutron study, and the lower end of the yield range from the Behrisch study, all agree within roughly a factor of 2. However, the Harling *et al.* yield with (d,Be) neutrons is about an order of magnitude lower. This rather large discrepancy is unexplained.

The approximate agreement between sputtering yields of fission- and fusion-energy neutrons, scaled by calculated damage-energy cross sections, indicates that the dominant mechanisms of sputtering do not differ greatly among the three neutron sources investigated. Agreement may even be improved with the higher flux levels attainable from future (d,T) and (d,Be) neutron sources. However, our current fission-neutron sputtering results support the claim that neutron sputtering will not be a major factor in erosion of the first containment wall in controlled thermonuclear reactors.

B. Possible mechanisms of sputtering

For the purpose of further discussion and comparison with sputtering theories, we will consider in turn the possible mechanisms for three types of sputtering, i.e., directional, cascade, and thermal-spike sputtering.

1. Directional sputtering

The directional sputtering mechanisms to be considered here are those that result in the emission of sputtered atoms along or near major crystallographic directions of bombarded face-centered-cubic crystals. The experimental observation of spot patterns associated with this type of sputtering is discussed extensively by Nelson.[24] These patterns have been observed for light- and intermediate-mass ion bombardments of single crystals, especially for proton backsputtering in gold,[25] and were initially interpreted as evidence for very-long-range focused collision sequences (FCS), predominately in ⟨110⟩ directions. Alternatively, these spot patterns may be interpreted as the result of atom collisions in the first few atomic layers, without invoking a focusing mechanism.[26] This issue is not fully resolved, but recent experimental evidence suggests that ranges

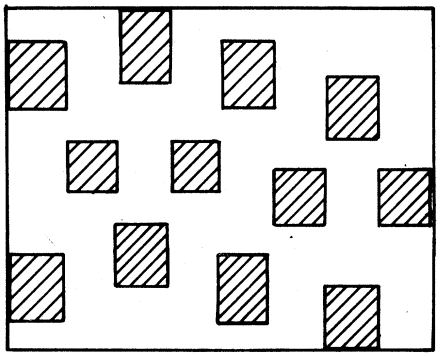

FIG. 6. Schematic of pattern for ⟨110⟩ directional sputtering in run *A*. Shaded rectangles are projections of the gold crystal onto the cylindrical collector in the 12 ⟨110⟩ directions for the particular crystal orientation in this run. Cylindrical axis is vertical.

of ⟨110⟩ FCS are no longer than[27] 5 to[28] 15 nm in gold.

The geometry of our experiment was designed in part to resolve a sputtering pattern consisting, to some degree, of ⟨110⟩ spots. A schematic of this type of sputtering spot pattern for the crystal orientation of run *A* is shown in Fig. 6. As mentioned earlier, no such pattern was resolved by autoradiography with visual inspection, or by densitometer scans of the entire autoradiograph (a more sensitive technique). Since at least 85% of the total sputtering yield was found to be caused by random sputtering, a maximum of 15% of the yield could be attributed to directional sputtering. Even though this fraction of the yield would have been easily resolved had it been included in the ⟨110⟩ spot pattern of Fig. 6, we will use 15% as an upper limit for the estimates and conclusions to follow.

The recoil and damage-energy distributions for gold in our neutron spectrum were calculated with the DISCS code and are displayed in Table III.[29] The damage-energy distribution shown in Table III was calculated using Robinson's approximate analytical expressions[30] for the Lindhard *et al.* theory.[31]

We first consider the possible directional sputtering caused by recoil events in the very-near-surface region (about three atom layers). To provide directional sputtering in ⟨110⟩ directions, we restrict our attention to recoils with energies <400 eV. A simple calculation shows that the maximum contribution of such recoils to sputtering is roughly three orders of magnitude below the 15% yield conservatively attributed to directional sputtering. We are thus not able to detect this surface mechanism for directional sputtering. We conclude that, directional or not, these very-near-surface recoil events make a negligible contribution to the

TABLE III. Primary recoil and damage-energy distribution for gold in the cryogenic fast-neutron-irradiation facility in CP-5.

Recoil-energy group	Primary recoils (%)[a]	Error (%)[b]	Damage energy (%)[c]
5–10 eV	5.8	17.4	0.02
10–20 eV	6.3	17.8	0.04
20–50 eV	7.6	9.4	0.1
50–100 eV	6.1	6.2	0.2
100–200 eV	8.1	8.3	0.5
200–400 eV	10.6	9.4	1.2
400–600 eV	7.2	10.8	1.4
600–800 eV	5.3	13.5	1.4
800–1000 eV	4.2	16.4	1.5
1–1.5 keV	7.4	20.9	3.6
1.5–2 keV	4.8	27.3	3.2
2–3 keV	6.1	27.4	5.7
3–5 keV	6.5	23.2	9.5
5–7 keV	3.4	16.7	7.4
7–10 keV	2.9	14.0	8.9
10–20 keV	4.4	11.0	22.6
20–40 keV	2.4	5.2	22.3
40–60 keV	0.4	5.1	6.2
60–80 keV	0.1	5.1	2.0
80–100 keV	0.04	7.2	1.2
>100 keV	0.2		0.9

[a] Total primary recoil cross section, 8.95 (±10.9%) b with minimum recoil energy of 5 eV (14.6 b if only neutrons with $E \geq 0.1$ MeV are considered).

[b] One standard deviation of recoils within a group, expressed as percent of recoils within that group.

[c] Total damage-energy cross section, 19.82 (±8.7%) keV b (32.4 keV b if only neutrons with $E \geq 0.1$ MeV are considered).

fast-neutron sputtering yield.

Focused collision sequences could make a significant contribution to directional sputtering during fast-neutron bombardment if the probability of FCS occurrence per recoil and average FCS range were both sufficiently large. To obtain an estimate of this effect consistent with the results of the present experiment, we assume the maximum yield (15% of the total) for nonrandom sputtering and calculate the average FCS length needed to produce this yield. Initially, we consider recoils with energies below 600 eV. This allows us to use the results of other experiments in this energy range. About 50% of the total recoils for gold in our facility have energies below 600 eV (Table III). In this energy range the probability of forming a long FCS in gold has been estimated at 10^{-3} (Ref. 27) to 10^{-4} (Ref. 28) per recoil. Based on a value of 10^{-3} for this probability, a simple calculation shows that an average FCS length of about 60 μm is necessary to account for 15% of the total measured yield. In the high-energy half of the recoil spectrum, the probability of FCS formation per primary recoil is not likely to be any larger than 10^{-3}; it may, in fact, be even smaller, based on results in Ni_3Mn.[32] Therefore, considering the entire energy spectrum of recoils in gold, FCS ranges of the order of 10 μm are needed to produce the 15% of total yield that can be experimentally attributed to directional sputtering. An FCS range in gold of 10 μm is roughly three orders of magnitude larger than that measured by Ecker[27] or Ayrault *et al.*[28] Thus it seems unreasonable to assume that even 15% of our sputtering yield can be attributed to directional sputtering caused by an FCS mechanism. Given an FCS range of 10 nm (the upper limits found by Ecker and Ayrault *et al.* are 5 and 15 nm, respectively), the fractional contribution of directional sputtering to our total sputtering yield is roughly 10^{-4}. Based on these calculations, the total sputtering yield we measured must be attributed to a random sputtering mechanism that results from the intersection of high-energy recoil cascades with the surface; this will be discussed in the following subsections.

2. *Cascade sputtering*

The most recent analytical theory of sputtering, and the one with which the present experimental results will be compared, has been proposed by Sigmund.[11] Using linear Boltzmann transport theory, he calculated sputtering yields for amorphous materials for a wide variety of experiments. This

theory has shown good agreement with numerous ion-backsputtering and transmission-sputtering experiments.[33] One notable exception to this good agreement has been found in sputtering experiments with high-energy (50-keV to 1-MeV), high-Z ion bombardment of high-Z targets.[34] This occurrence of so-called nonlinear effects may also have some application to the present results (see Sec. III B 3).

Sigmund's expression for the sputtering ratio of a sample in an isotropic neutron flux is exactly given as

$$S = 2g\Lambda N\sigma\langle\nu(E)\rangle, \tag{2}$$

where g is a geometrical factor equal to unity for a spherical sample and Λ is a constant characterizing the sample material with atomic density N. We can identify the product of the cross section (σ) and average damage energy ($\langle\nu(E)\rangle$) with the previously defined spectrum-averaged damage-energy cross section $\langle\sigma T_d\rangle$. [This had already been done in Eq. (1).] For comparison with the present experiment, we can simplify the above expression to include only the essential parameters of interest; this gives

$$S = 0.084\langle\sigma T_d\rangle/U_0, \tag{3}$$

where U_0 is the surface binding energy in eV and $\langle\sigma T_d\rangle$ is given in Å^2 eV.

The surface binding energy U_0 is usually taken to be equal to the sublimation energy, which for gold is 3.8 eV.[35] However, recent experimental evidence based on the threshold of transmission sputtering by high-energy electrons suggests a value for U_0 of 5–6 eV.[36] Therefore, to account for these uncertainties we take $U_0 = 5(\pm 1)$ eV.

As shown in Table III (footnote c), the value of $\langle\sigma T_d\rangle$ calculated in our neutron spectrum, and defined for the integrated flux above neutron energies of 0.1 MeV, is 32.4 bkeV (32.4×10^{-5} Å^2 eV). We do not incorporate the absolute error (based on the neutron-spectrum error) in this value, since we are comparing experiment and theory for the same neutron spectrum. Thus the theoretical prediction of Sigmund's sputtering ratio for a spherical target in our isotropic flux is $S = (5.4 \pm 1.1) \times 10^{-6}$ atoms per incident neutron ($E > 0.1$ MeV). The experimentally determined sputtering ratio [$S = (1.2 \pm 0.4) \times 10^{-5}$, Table II], is roughly a factor of 2 greater than the theoretical value. This disagreement, though not substantial relative to the wide range of other experimental results, is nonetheless outside the relative uncertainties of the present experimental and theoretical values, and may therefore be significant. Possible reasons for this discrepancy will be suggested in Sec. III B 3.

Sigmund's theory of neutron sputtering is based on the intersection of the recoil cascade with a surface (resulting in the emission from the surface layer of those atoms with energies exceeding U_0), averaged over all possible events defined by the recoils that make significant contributions to the damage-energy distribution shown in Table III. Assuming a representative recoil at 50% of the damage-energy distribution (approximately 12 keV), and using the calculated projected range of 2.5 nm (Ref. 37) for a 12-keV gold ion in gold, the approximate number of sputtered atoms per representative near-surface cascade may be calculated. Considering only recoils with energy >1 keV (which include 94% of the damage-energy distribution), the cross section to be used will be ~40% of the total recoil cross section above 5 eV (14.6 b), or 5.9 b. The result of this calculation, for the experimental sputtering ratio of 8.0×10^{-6} sputtered gold atoms per incident neutron, is ~100 sputtered gold atoms per representative near-surface cascade.

Some speculation is possible as to why the experimental sputtering distribution is narrower than random sputtering (Fig. 3). A surface structure, irregular on an atomic scale, might contribute to a narrowing. However, the physical mechanism of sputtering itself might also be the cause. Within the linear cascade-sputtering theory, an anisotropy of U_0 would decrease the emission probability of atoms at low angles with the surface.[38] Beyond the linear cascade-sputtering theory, collective interactions among simultaneously sputtered surface atoms may produce a distribution weighted toward directions more perpendicular to the surface. Finally, sputtering of atoms from below the surface layer by thermal-spike effects would also produce a distribution narrower than random. Any or all of these mechanisms may be present during sputtering. Further discussions of the last one follows in Sec. III B 3.

3. *Thermal-spike sputtering*

The discrepancy between the experimental sputtering ratio of gold subjected to fast-neutron irradiation, as reported in the present work, and the sputtering ratio derived by Sigmund with a linear Boltzmann transport equation may be due to the nonlinear effects of interactions among moving atoms. The work of Bay *et al.*[39] suggests that these nonlinear or thermal-spike effects are present in the high-energy (100–1000 keV) gold-ion bombardment of gold, which results in sputtering yields two to three times greater than those predicted by Sigmund's theory. The lowest energy (45 keV) for which data are available on the gold-

ion bombardment of gold[40] gives a sputtering yield of almost twice that predicted by Sigmund's theory. In the present experiment, >90% of the damage energy for gold was found in primary recoils with energies <45 keV (see Table III), with the median damage energy at a primary recoil energy of 12 keV.

Because of this difference in energy ranges between ion sputtering and fast-neutron sputtering, the interpretation of thermal-spike effects in the former cannot be readily transferred to the latter. However, it is important to note that the intersection of a surface with the average recoil cascade (or distribution of cascade-surface intersections) is different for ion as compared with fast-neutron sputtering. The average cascade-surface intersection in the neutron sputtering case will probably sample the recoil cascade nearer the cascade center than in the ion sputtering case. This could lead to a stronger thermal-spike effect in neutron sputtering than in ion sputtering at comparable primary recoil energies. Therefore, the contribution of thermal-spike effects to the fast-neutron sputtering of gold will be considered as a possible explanation for the discrepancy between experiment and linear-cascade theory.

For thermal-spike effects to make a significant contribution to sputtering, the energy density within the recoil cascade must be sufficiently high (>5 eV per atom) over a reasonable volume, and this high energy density must persist for a sufficient time to allow thermal sputtering to take place. Sputtering in random directions, as indicated by the autoradiograph of Fig. 2, is evidence of a high energy density within recoil cascades intersecting the surface during fast-neutron bombardment. Considering the intersection of high-energy recoil cascades with the surface, sputtering in crystalline directions by surface recoils or very short FCS's within the cascade might be possible. However, the fact that the neutron sputtering of gold is not influenced by crystal structure suggests that during the cascade lifetime the crystal structure is lost, as if melting had occurred within the cascade volume. Similar evidence for this loss of crystal structure has been observed by Nelson for 50-keV gold-ion bombardment of gold.[41]

Though no theory of sputtering by thermal spikes has been developed in enough detail to permit a calculation of predicted yields, some guidelines have been approximately calculated by Sigmund.[42] From the spatial distribution of deposited energy in elastic-collision cascades,[43] he has derived parameters to express the effective maximum energy density within the typical cascade. For gold, the energy density exceeds 5 eV per atom for primary recoil energies below 100 keV. This is sufficient to permit thermal sputtering in the present experiment provided, as Sigmund proposes, the spike lifetime exceeds the cascade lifetime or the slowing-down time of the primary recoil. Calculations of the appropriate lifetimes are displayed in Fig. 7, along with the distribution of damage energy for gold in the present neutron spectrum. The cascade lifetime or slowing-down time for a gold primary recoil is calculated from the work of Oen and Robinson.[44] The thermal-spike lifetime for gold is calculated from Sigmund's equations on the basis of kinetic gas theory.[42] From the data and calculations in Fig. 7, sputtering due to thermal-spike effects must be caused by recoils between ~20 and 100 keV, where 30% of the damage energy is found. This may not be a sufficient fraction of the damage-energy distribution to provide the needed thermal sputtering; thus Sigmund may be underestimating the thermal-spike lifetime. In this regard, a thermal sputtering theory recently developed by Kelly,[45] based on an approximate solution of the heat-conduction equation in a solid, appears to give somewhat longer effective lifetimes for thermal spikes. However, calculations applicable to experiments are yet to be published by Kelly.

Since the disagreement between the present experimental sputtering ratio and that calculated by linear cascade theory is just outside the uncertainties in both, this suggestion of a thermal spike contribution to the sputtering of gold by fast neutrons must be considered somewhat tentative. However, the same mechanism is now being con-

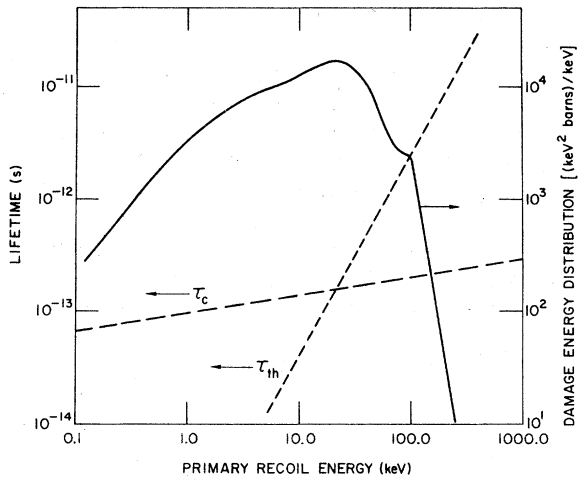

FIG. 7. Cascade lifetime (τ_c) and thermal-spike lifetime (τ_{th}) vs primary-recoil energy in gold, as calculated by Oen and Robinson (Ref. 44) and Sigmund (Ref. 42), respectively. Also plotted is the damage-energy distribution for gold in our neutron-energy spectrum vs primary-recoil energy.

sidered to contribute to efficiencies (relative to modified Kinchin and Pease theory[46]) less than unity for Frenkel-defect production in high-energy collision cascades.[47] Additional fast-neutron sputtering experiments are needed to clarify this point.

Finally, an observation made by Merkle[48] should be mentioned. Following 100-keV gold-ion bombardment of gold foils, small craters were observed to intersect the foil surface. These were associated with a small fraction of cascades (actually subcascade clusters) produced throughout the foil. Based on the estimated crater volume, ~1000 atoms were apparently sputtered from a typical crater. Though this recoil energy is too high to be of significance in the present distribution of recoils in gold for fast-neutron irradiation, this may be an observation of a rather strong thermal-spike effect due to recoils in gold near 100 keV. Subcascades formation is not expected to be important in the present results, however, since Merkle measures this to be negligible below a recoil energy of about 30 keV in gold,[49] an energy range that accounts for about 85% of the sputtering in the present study.

IV. SUMMARY

Experiments on the sputtering of single-crystal gold by fast neutrons have been described. The gold crystals were activated in a thermal-neutron flux prior to sputtering in the cryogenic fast-neutron-irradiation facility at the CP-5 reactor. Sputtering took place in a vacuum of better than 10^{-6} Torr (0.13 mPa) and at a temperature of <40 K. Prior activation permitted the resolution of the spatial distribution of sputtered atoms by autoradiographic techniques, and also permitted a more accurate total-yield determination by γ counting. Accurate background subtractions and semiquantitative corrections for small amounts of contamination were possible with this method. A detailed determination of the neutron flux and energy spectrum was accomplished, along with a calculation of damage parameters for gold.

The autoradiographic results showed a nearly random spatial distribution of sputtered atoms. An average sputtering ratio of 8.0×10^{-6} sputtered gold atoms per incident neutron ($E > 0.1$ MeV) was found with an absolute error of ±34%.

An extensive comparison with other results on fast-neutron sputtering of gold was accomplished by normalizing all results to similar geometry and our neutron-spectrum-averaged damage-energy cross section for gold. The present results with fission neutrons agreed, within a factor of 2, with the most recent results for (d, T) and (d, Be) neutrons. This indicates that the dominant mechanisms of sputtering are similar for these three neutron-energy spectra.

The results of this experiment are discussed with respect to three possible mechanisms of sputtering. It is concluded that directional sputtering by focused collision sequences does not contribute significantly to the measured sputtering yield; rather, this yield must be attributed to a random sputtering mechanism based on the high-energy recoil cascades that intersect the surface. However, a calculation of the sputtering ratio to be expected in our neutron spectrum on the basis of Sigmund's linearized Boltzmann transport theory yields approximately half of our experimental value. It thus may be necessary to include a nonlinear or thermal-spike contribution to the total sputtering yield to account for this difference.

ACKNOWLEDGMENTS

The authors would like to express their appreciation to A. Gabriel (ORNL) and D. Parkin(LASL) for performing calculations of primary recoil atom distributions with our neutron spectrum. We wish to thank T. L. Scott for his assistance at the cryogenic irradiation facility. The help of the CP-5 reactor personnel was essential and was greatly appreciated by us. We are very grateful to A. Jackowski for his vital assistance with the hot-cell work. The advice and support of T. H. Blewitt is warmly acknowledged. Thanks to S. J. Rothman (ANL), R. S. Averback (ANL), and G. R. Odette (University of California, Santa Barbara), for discussions and critical readings of the manuscript. This work was supported by the Basic Energy Sciences Division of the U. S. Department of Energy.

---

[1]M. A. Kirk, T. H. Blewitt, A. C. Klank, T. L. Scott, and R. Malewicki, J. Nucl. Mater. 53, 179 (1974).

[2]M. A. Kirk and R. A. Conner, in *Proceedings of the International Conference on Fundamental Aspects of Radiation Damage in Metals*, edited by M. T. Robinson and F. W. Young (USERDA, Oak Ridge, 1976), Vol. 1, p. 171.

[3]C. O. Muehlhause, M. Ganoczy, and C. Kupiec, IEEE Trans. Nucl. Sci. 12, 478 (1965).

[4]Run *A* was reported in preliminary fashion in Ref. 2 using an incorrect fluence, as the more accurate and detailed flux determination described in Sec. IID had not been accomplished at that time.

[5]T. H. Blewitt and T. J. Koppenaal, in *Radiation Effects*,

edited by W. F. Sheely (Gordon and Breach, New York, 1966), p. 561.
[6]A. C. Klank. T. H. Blewitt, J. J. Minarik, and T. L. Scott, Bull. Inst. Int. Froid Suppl. 5, 373 (1966).
[7]W. N. McElroy, S. Berg, T. B. Crockett, and R. J. Tuttle, Nucl. Sci. Eng. 36, 15 (1969).
[8]R. I. Garber, G. P. Dolya, V. M. Kolyada, A. A. Modlin, and A. I. Fedorenko, JETP Lett. 7, 296 (1968).
[9]B. P. Fairand, Ph.D. thesis (Ohio State University, 1969) (unpublished).
[10]W. O. Hofer, Radiat. Eff. 21, 141 (1974).
[11]P. Sigmund, Phys. Rev. 184, 383 (1969).
[12]In a mixed spectrum of fast and thermal neutrons Norcross *et al.* (Ref. 14) and Fairand (Ref. 9) found the sputtering contribution of the thermal-neutron (n,γ) recoils to be negligible.
[13]An alternate approach would be to redefine the experimental sputtering ratio as the number of sputtered atoms per damage-energy dose $(nvt < \sigma E_d >)$.
[14]D. W. Norcross, B. P. Fairand, and J. N. Anno, J. Appl. Phys. 37, 621 (1966).
[15]G. R. Odette and D. R. Doiron, Nucl. Tech. 29, 346 (1976).
[16]J. B. Roberto, M. T. Robinson, and C. Y. Fu, J. Nucl. Mater. 63, 460 (1976).
[17]K. Verghese, Trans. Am. Nucl. Soc. 12, 544 (1969).
[18]R. Behrisch, Nucl. Instrum. Methods 132, 293 (1976).
[19]R. Behrisch, R. Gähler, and J. Kalus, J. Nucl. Mater. 53, 183 (1974).
[20]R. Gähler, diplomarbeit (Technische Universität München, 1974) (unpublished).
[21]O. K. Harling, M. T. Thomas, R. L. Bradzinski, and L. A. Rancitelli, J. Nucl. Mater. 63, 422 (1976).
[22]L. H. Jenkins, G. L. Smith, J. F. Wendelken, and M. J. Saltmarsh, J. Nucl. Mater. 63, 438 (1976).
[23]L. Cranberg, C. Frye, N. Nereson, and L. Rosen, Phys. Rev. 103, 662 (1956).
[24]R. S. Nelson, *The Observation of Atomic Collisions in Crystalline Solids* (North-Holland, Amsterdam, 1968).
[25]R. S. Nelson and M. W. Thompson, Proc. R. Soc. Lond. 259, 458 (1960).
[26]C. Lehmann and P. Sigmund, Phys. Status Solidi 16, 507 (1966).
[27]K. H. Ecker, Radiat. Eff. 23, 171 (1974).
[28]G. Ayrault, R. S. Averback, and D. N. Seidman, Scr. Metall. 12, 119 (1978).
[29]These calculations agreed quite well with the results of similar calculations performed by A. Gabriel (unpublished) of Oak Ridge National Laboratory and D. Parkin (unpublished) of Los Alamos Scientific Laboratory using our neutron spectrum.
[30]M. T. Robinson, in *Nuclear Fusion Reactors*, edited by J. L. Hall and J. H. C. Maple (British Nuclear Energy Society, London, 1970), p. 364.
[31]J. Lindhard, V. Nielsen, M. Scharff, and P. V. Thomsen, K. Dan. Vidensk. Selsk. Mat.-Fys. Medd. 33, No. 10 (1963).
[32]M. A. Kirk, T. H. Blewitt, and T. L. Scott, J. Nucl. Mater. 69/70, 780 (1978).
[33]H. H. Andersen, in *Physics of Ionized Gases* 1974, edited by V. Vujnović (Institute of Physics of the University of Zagreb, Yugoslavia, 1974), pp. 361–426.
[34]H. H. Andersen and H. L. Bay, J. Appl. Phys. 46, 2416 (1975).
[35]K. Gschneidner, Solid State Phys. 16, 344 (1964).
[36]D. Cherns, M. W. Finnis, and M. D. Matthews, Philos. Mag. 35, 693 (1977).
[37]H. E. Schiott, Radiate. Eff. 6, 107 (1970).
[38]D. P. Jackson, Can. J. Phys. 53, 1513 (1975).
[39]H. L. Bay, H. H. Andersen, W. O. Hofer, and O. Nielsen, Nucl. Instrum. Methods 132, 301 (1976).
[40]O. Almén and G. Bruce, Nucl. Instrum. Methods 111, 179 (1961).
[41]R. S. Nelson, Radiate. Eff. 7, 263 (1971).
[42]P. Sigmund, Appl. Phys. Lett. 25, 169 (1974).
[43]K. B. Winterbon, P. Sigmund, and J. B. Sanders, K. Dan. Vidensk. Selsk. Mat.-Fys. Medd. 37, No. 14 (1970).
[44]O. S. Oen and M. T. Robinson, J. Appl. Phys. 46, 5069 (1975).
[45]R. Kelly, Radiate. Eff. 32, 91 (1977).
[46]M. J. Norgett, M. T. Robinson, and I. M. Torrens, Nucl. Eng. Design 33, 50 (1974).
[47]R. S. Averback, R. Benedek, and K. L. Merkle, J. Nucl. Mater. 75, 97 (1978).
[48]K. L. Merkle, in *35th Annual Proceedings of the Electron Microscopy Society of America*, edited by C. W. Bailey (Claytors, Baton Rouge, LA, 1977), p. 36.
[49]K. L. Merkle, in *Radiation Damage in Metals*, edited by N. L. Peterson and S. D. Harkness (American Society for Metals, Metals Park, Ohio, 1976), p. 75.

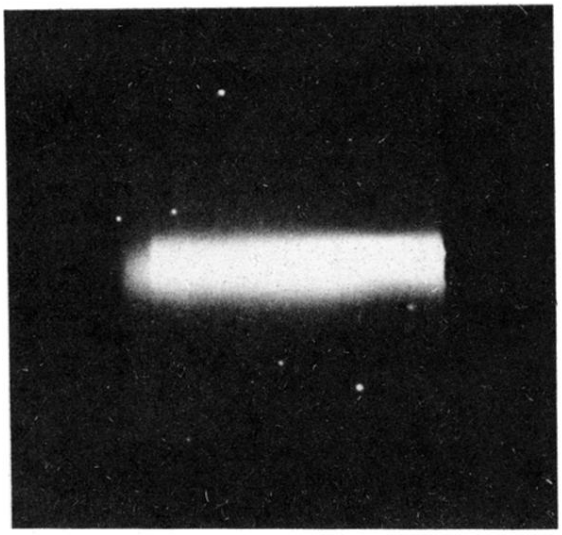

FIG. 2. Positive print of autoradiograph of collector foil from run *A* (cylindrical axis is vertical).